Available online at www.sciencedirect.com
SCIENCE DIRECT®
Bioorganic & Medicinal Chemistry 12 (2004) 3289–3298
Bioorganic & Medicinal Chemistry

Parallel synthesis of a library of bidentate protein tyrosine phosphatase inhibitors based on the α-ketoacid motif ☆

Yen Ting Chen and Christopher T. Seto*

Department of Chemistry, Brown University, 324 Brook St. Box H, Providence, RI 02912, USA

Received 2 February 2004; revised 25 March 2004; accepted 26 March 2004
Available online 10 May 2004

Abstract—Protein tyrosine phosphatases (PTPases) regulate intracellular signal transduction pathways by controlling the level of tyrosine phosphorylation in cells. These enzymes play an important role in a variety of diseases including type II diabetes and infection by the bacterium *Yersinia pestis*, which is the causative agent of bubonic plague. This report describes the synthesis, using parallel solution-phase methods, of a library of 104 potential inhibitors of PTPases. The library members are based on the bis(aryl α-ketocarboxylic acid) motif that incorporates a carboxylic acid on the central benzene linker. This carboxylic acid was coupled with a variety of different aromatic amines through an amide linkage. The aromatic component of the resulting amides is designed to make contacts with residues that surround the active site of the PTPase. The library was screened against the *Yersinia* PTPase and PTP1B. Based upon the screening results, four members of the library were selected for further study. These four compounds were evaluated against the *Yersinia* PTPase, PTP1B, TCPTP, CD45, and LAR. Compound **14** has an IC_{50} value of 590 nM against PTP1B and is a reversible competitive inhibitor. This affinity represents a greater than 120-fold increase in potency over compound **2**, the parent structure upon which the library was based. A second inhibitor, compound **12**, has an IC_{50} value of 240 nM against the *Yersinia* PTPase. In general, the selectivity of the inhibitors for PTP1B was good compared to LAR, but modest when compared to TCPTP and CD45.

1. Introduction

Protein tyrosine phosphatases (PTPases) and kinases regulate the level of tyrosine phosphorylation of proteins, and as a result they are one of the key mechanisms for controlling intracellular signal transduction pathways. The unregulated activity of phosphatases is associated with a variety of diseases.[1,2] For example, PTP1B dephosphorylates the insulin receptor and a number of downstream signaling proteins, and is thus a potential target for the treatment of type II diabetes.[3–5] Several PTPases including PTP-α and the Cdc25 phosphatases are implicated in the development of cancer. PTP-α activates the Src-family of kinases while Cdc25B activates the cyclin-dependent kinases.[6] CD45 is a potential target for the treatment of autoimmune diseases and inflammation because it is involved with the activation of B and T cell receptor signaling.[7] Finally, bacterial infection by *Yersinia pestis*, the agent that is responsible for the bubonic plague, relies on the activity of a PTPase (YopH). This pathogenic bacterium secretes the phosphatase into host cells, where it disrupts host signal transduction processes and thus interferes with the immune response.[8] Since PTPases are important in such a wide variety of biological processes, there is currently significant interest in these enzymes as targets for therapeutic intervention and a great deal of effort is being invested toward the development of potent and specific PTPase inhibitors that also show good bioavailability.

Because all PTPases share a common catalytic mechanism, and many of them have a highly conserved active site,[9] one of the most challenging aspects of designing inhibitors for these enzymes is the ability to achieve selectivity for one particular PTPase over others. The active site of PTPases is selective for binding phosphotyrosine.[10] However, phosphotyrosine by itself has a low affinity for the enzyme. Thus, it is apparent that regions of the active site cleft beyond the catalytic residues are crucial for efficient recognition and binding of

Keywords: Phosphatase; Inhibitor; Library; α-Ketocarboxylic acid.
☆ Supplementary data associated with this article can be found, in the online version, at doi:10.1016/j.bmc.2004.03.058
* Corresponding author. Tel.: +1-401-863-3587; fax: +1-401-863-9368; e-mail: christopher_seto@brown.edu

0968-0896/$ - see front matter © 2004 Elsevier Ltd. All rights reserved.
doi:10.1016/j.bmc.2004.03.058

substrates.[11] Zhang and co-workers have identified residues in PTP1B (Arg-24, Arg-254, Gln-262) that comprise a secondary binding site that is near to the catalytic site.[12] These investigators reasoned that, by the principle of additivity of the free energy of binding, inhibitors that bind in both the catalytic site and the secondary site should have significantly increased affinity for the enzyme. This notion is supported by studies involving the biphosphorylated insulin receptor kinase (IRK) activation loop that is a substrate for PTP1B. The crystal structure of the enzyme–substrate complex shows that the two phosphotyrosine residues in the substrate bind simultaneously to both sites. In addition, the biphosphorylated substrate has a much greater affinity for PTP1B than its monophosphorylated analog.[13] Since the residues that comprise the secondary site are not conserved among all PTPases, it is reasonable to expect that dual-binding inhibitors will exhibit increased selectivity, as well as increased affinity.

Several groups have taken advantage of this concept and reported inhibitors that contain two phosphotyrosine mimics, such as aryl difluoromethylenephosphonates, which are tethered together by a linker.[14–16] These compounds display significantly improved inhibition and selectivity when compared to inhibitors that bear only a single phosphotyrosine mimic. They generally have inhibition constants against PTP1B that range from low micromolar to as low as 2 nM. However, structural studies have revealed that many of these bidentate inhibitors make contacts with the active site and other less conserved, neighboring residues such as Lys-41, Arg-47, and Asp-48, rather than the secondary binding site.[17–19] Recently, a group from Abbott Laboratories used a linked-fragment strategy to generate several potent oxalylamide-based inhibitors. These investigators used X-ray crystallography to confirm that the inhibitors occupy both the catalytic site and the secondary binding site.[20] Taken together, these results suggest that targeting a combination of the active site and either the secondary binding site or Arg-47 and Asp-48 are both effective strategies for developing PTPase inhibitors.

Over the past several years, we have been working to develop aryl α-ketocarboxylic acids as inhibitors of PTPases.[21,22] By linking two or three aryl α-ketoacids to a central aromatic core, we demonstrated that the potency of the inhibitors against the *Yersinia* PTPase can be increased up to 280-fold when compared to monomeric α-ketoacids such as 4-hydroxyphenylglyoxylic acid (**1**). Of the multivalent compounds that we have studied, compound **2** showed the highest activity against the *Yersinia* PTPase and PTP1B, and it had good selectivity for these enzymes over LAR.[23] This inhibitor has an IC_{50} value of 2.7 μM against PTP1B at pH 5.5. However, the binding affinity decreases significantly ($IC_{50} = 73$ μM) when the assays are performed at pH 7.0. Since LAR does not possess the residues that form the secondary site,[12] one reasonable interpretation of these inhibition data is that compound **2** may be binding to both the active site and the secondary site. However, modeling studies suggest that compound **2** may be more likely to bind to the active site and Arg-47

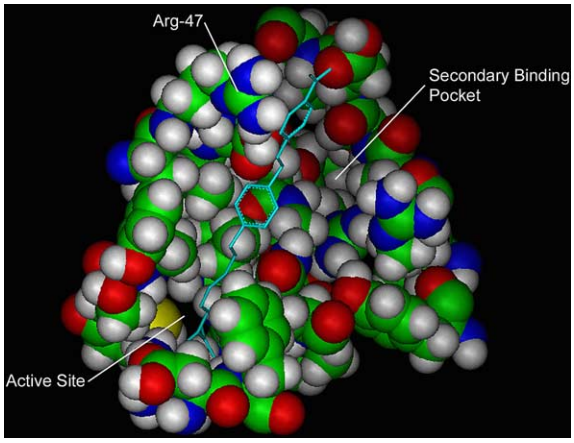

Figure 1. Computer generated model of compound **2** bound in the active site of PTP1B.

of PTP1B (Fig. 1), rather than the secondary site. An Arg residue is present in an analogous position in the *Yersinia* PTPase, but not in LAR. The model shown in Figure 1 illustrates that, while the inhibitor can bind with one α-ketoacid unit anchored in the active site and the other extended toward Arg-47 and Asp-48, in this conformation it does not take advantage of binding interactions with the secondary site. As a result, we may be able to improve the potency and selectivity of the inhibitor by building on additional functionality to the central benzene core that could extend into the secondary site. Here, we report on the synthesis and screening of a 104-membered library of inhibitors with the general structure **3**. These compounds are based on the structure of inhibitor **2**, with the addition of a carboxylic acid group that is appended to the central benzene ring. Coupling reactions between this carboxylic acid and a variety of aromatic amines were used to generate the library.

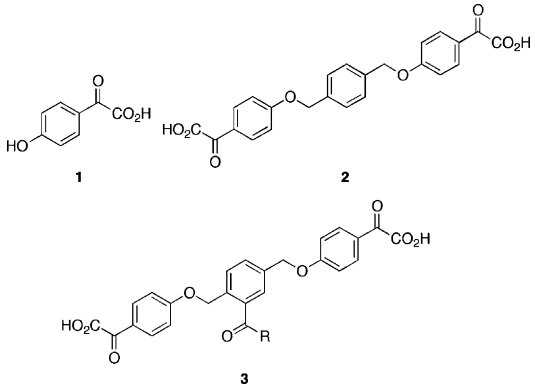

2. Results and discussion

2.1. Chemistry

In our previous studies, we employed a transamination procedure using copper sulfate and glyoxylic acid to convert esters of α-amino acids into the corresponding α-ketoesters. These were subsequently hydrolyzed to

yield α-ketocarboxylic acids.[23] Although the transamination reaction reliably provided the desired products, the yields for this transformation were generally poor. In order to avoid this problem, we have adopted a new strategy for the synthesis of α-ketoacids in which α-amino acids are first treated with trifluoroacetic anhydride to give the corresponding trifluoromethyloxazolones following the procedure of Barnish et al.[24] The trifluoromethyloxazolone, which serves as a protecting group, can be hydrolyzed at the end of the synthesis to yield the corresponding α-ketoacid.

This strategy is illustrated in Scheme 1, which begins with a Williamson ether synthesis using 1 equiv of compound **4** and 2 equiv of **5** to give **6**. This reaction was performed using sodium ethoxide in ethanol as the base. These conditions also promoted a transesterification reaction that converted the methyl ester group in **5** into an ethyl ester. The synthesis of compounds **4** and **5** have been reported previously.[23,25] The Boc protecting groups in compound **6** were removed with trifluoroacetic acid to yield amine **7**. Next, the three ester groups in **7** were hydrolyzed using aqueous sodium hydroxide to give amino acid **8**. Refluxing compound **8** in trifluoroacetic anhydride gave bis-oxazolone **9**. Compared to the transamination protocol, the oxazolone procedure requires an additional step, but gives an overall yield that is significantly higher.

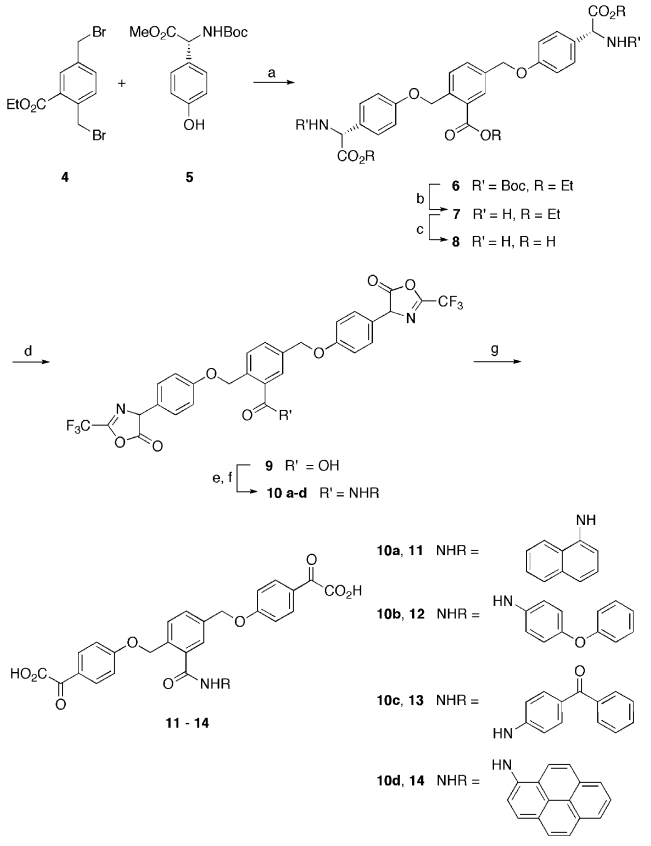

Scheme 1. Reagents and conditions: (a) Na, EtOH, 90%; (b) TFA, CH_2Cl_2, 91%; (c) NaOH, H_2O; (d) trifluoroacetic anhydride, 76% (two steps); (e) $SOCl_2$, benzene; (f) RNH_2, CH_2Cl_2 or THF; (g) NaOH, H_2O.

Reaction of compound **9** with thionyl chloride gave the corresponding acid chloride. The library of inhibitors was generated by reacting this acid chloride in parallel with 103 different commercially available aromatic amines (Fig. 2) to give amides with the general structure **10**. After the coupling reactions were judged to be complete by TLC analysis, the solvents were removed and the resulting amides (**10**) were treated with dilute sodium hydroxide to hydrolyze the two trifluoromethyloxazolone groups and unmask the final α-ketocarboxylic acids. Compound **9** was hydrolyzed in the same manner to give the corresponding α-ketoacid inhibitor with a carboxylic acid group on the central benzene ring, rather than an amide. The final products from these reactions were analyzed by LCMS to verify that the syntheses were successful. The inhibitors were screened in crude form, without purification, against the *Yersinia* PTPase and PTP1B. Following this initial screen, we selected four of the inhibitors (compounds **11**–**14**) for further evaluation. These inhibitors were resynthesized using the same chemistry, except that the trifluoromethyloxazolone intermediates **10a**–**d** were purified prior to the final hydrolysis reaction.

Several details concerning the synthesis of this library are worth noting. First, the trifluoromethyloxazolone group is unstable under basic conditions. As a result, we have limited the library to include only aromatic amines that generally are less basic than aliphatic amines. Reaction of the acid chloride derived from compound **9** with aliphatic amines such as benzylamine or diethylamine led to decomposition of the oxazolone groups as determined by LCMS and ^{19}F NMR analysis. No such decomposition was observed in coupling reactions with aromatic amines. Second, coupling reactions using compounds such as sulfanilic acid, which are insoluble in the reaction solvent (CH_2Cl_2 or THF), were not successful. Third, while coupling reactions with tetra- and pentafluoroaniline derivatives were successful, the resulting amides were hydrolyzed back the carboxylic acid during the hydrolysis of the trifluoromethyloxazolone groups. Finally, for library members that contained other base-labile functional groups such as an ethyl ester, benzothiazole, or phthalimide, these groups were also hydrolyzed during cleavage of the trifluoromethyloxazolones.

2.2. PTPase inhibition

We initially screened the library of inhibitors by determining the percent inhibition of the compounds against the *Yersinia* PTPase and PTP1B at 1 and 5 μM inhibitor concentrations, respectively (Figs. 3 and 4). These measurements were performed with *p*-nitrophenyl phosphate (*p*-NPP) as the substrate at 25 °C in 100 mM acetate buffer at pH 5.5. For reference, compound **A104**, which has a carboxylic acid rather than an amide on the central benzene ring of the inhibitor, gives 12% inhibition of the *Yersinia* PTPase at 1 μM concentration. This compound has a IC_{50} value of 13 μM at pH 5.5 against this enzyme. The 10 best inhibitors of the *Yersinia* PTPase are presented in Table 1, using the same

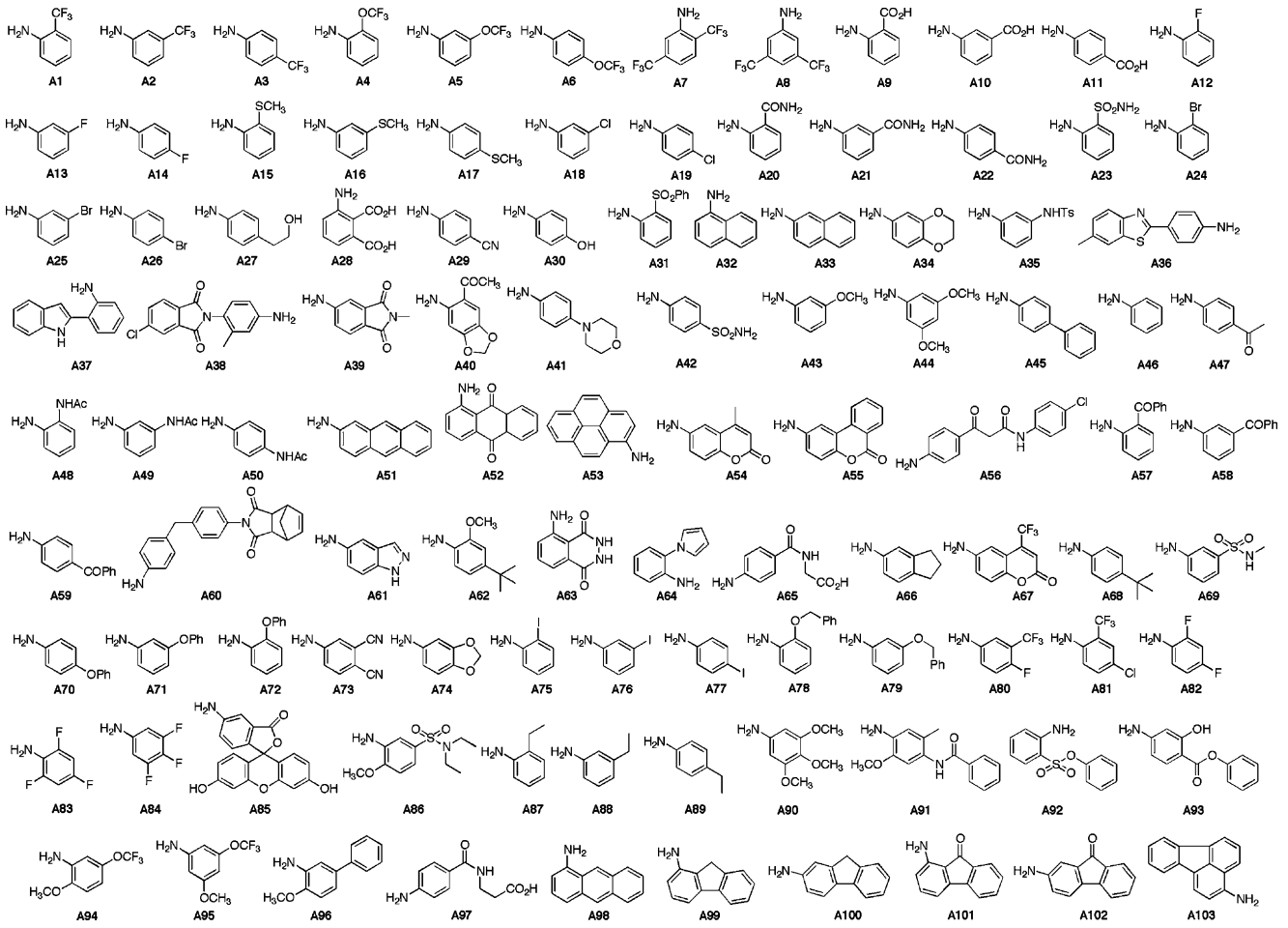

Figure 2. Aromatic amines used to synthesize the library. The designator under each aromatic amine refers to the library member with general structure **3** where the R component is derived from the above amines.

designators provided in Figure 2. In order to improve the dynamic range of the PTP1B assays, 16 of the best inhibitors of this enzyme were re-assayed at pH 5.5 at a concentration of 2 μM. The 10 best PTP1B inhibitors that emerged from this second round of assays, along with their % inhibition values, are shown in Table 2. The library members in Tables 1 and 2 share several common features. First, inhibitors that contain polycyclic aromatic groups such as naphthalene (**A32**), anthracene (**A51** and **A98**), and pyrene (**A53**) have good activity. Second, inhibitors derived from both *meta*- and *para*-phenoxyaniline (**A70** and **A71**) are prominent in both tables. Finally, the compound derived from 3-aminobenzoic acid (**A10**) is a good inhibitor of both the *Yersinia* PTPase and PTP1B. It is possible that the benzoic acid moiety is favorable because it can make electrostatic contacts with Arg-24 or Arg-254 in the secondary binding site of PTP1B and with homologous Arg residues in the secondary site of the *Yersinia* PTPase.

Based upon these initial screening results, we chose four inhibitors (**11**–**14**, corresponding to library members **A32**, **A70**, **A59**, and **A53**, respectively) to investigate in more detail. These compounds were resynthesized and purified using standard techniques. In order to evaluate the inhibitors under more physiologically relevant conditions and under conditions that provide a direct comparison with most of the recent studies published in the literature, we chose to perform the IC_{50} measurements of these compounds using 50 mM 3,3-dimethylglutarate buffer at pH 7.0 (Table 3). The four inhibitors were assayed against the *Yersinia* PTPase, PTP1B, LAR, CD45, and TCPTP.

Compounds **11**–**14** are all potent inhibitors of the *Yersinia* PTPase, with IC_{50} values that range from 240 to 670 nM. Like many of the previous α-ketoacid-based inhibitors that we have studied,[23] these compounds show greater potency against the *Yersinia* PTPase than PTP1B. Nevertheless, compound **14** in particular is a good inhibitor of PTP1B with an IC_{50} value of 590 nM. For comparison, compound **2** that is the parent structure upon which this library was constructed, has an IC_{50} value of 73 μM under the same conditions. Thus, our combinatorial strategy that was designed to fill the secondary binding site of PTP1B with an appropriate functional group, has lead to a more than 120-fold increase in the potency of the inhibitor. Lineweaver–Burk analysis of compound **14** confirms that it is a reversible, competitive inhibitor of PTP1B (Fig. 5).

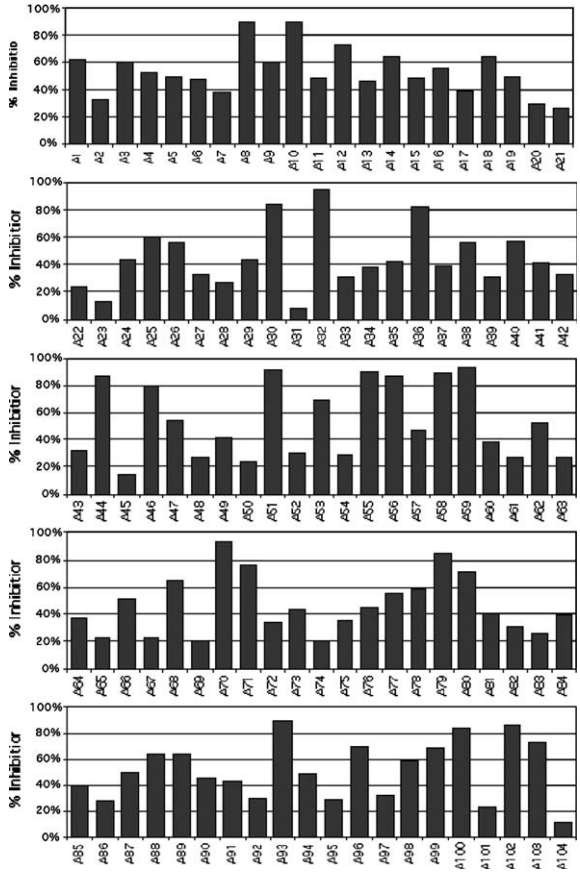

Figure 3. Assay of library members at 1 μM concentration against the *Yersinia* PTPase. Designators on the *x*-axis refer to the library members shown in Figure 2.

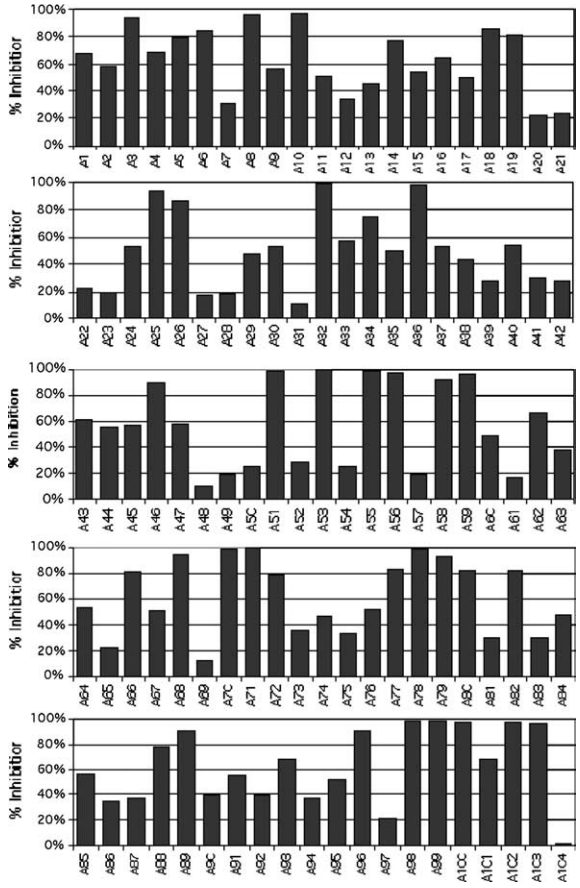

Figure 4. Assay of library members at 5 μM concentration against PTP1B. Designators on the *x*-axis refer to the library members shown in Figure 2.

Compounds **11**–**14** show less than a factor of two selectivity for PTP1B over TCPTP. TCPTP is a nontransmembrane PTPase like PTP1B and the *Yersinia* PTPase, and it is also the closest structural homologue to PTP1B.[26] These three phosphatases share many residues in common including those that make up the secondary binding site, and many other residues near the active site that are important for binding including Arg-47 and Asp-48. As a result, it is not surprising that the inhibitors show good affinity for both enzymes. The lack of selectivity between PTP1B and TCPTP is caused by the structural similarity of these two enzymes, since all the factors involved in binding of the inhibitors to PTP1B are also present in TCPTP. Among the numerous PTPase inhibitors that have been reported by other groups, only a few exhibit significant selectivity for PTP1B over TCPTP.[15,27,28]

LAR and CD45 are receptor type phosphatases that have a different architecture when compared to the nontransmembrane PTPases. Like PTP1B, LAR is involved in the control of insulin receptor signaling,[29] while CD45 is important in T cell regulation.[30] Inhibitors **11**–**14** have greater than 150-fold selectivity for PTP1B over LAR. LAR does not have a residue that corresponds to Arg-47 of PTP1B, and also lacks the residues that make up the secondary binding site. Because these residues play a key role in governing the binding interactions between enzyme and inhibitor and they are missing in LAR, the inhibitors should have weak affinity for LAR as is observed. In contrast compounds **11**–**14** are reasonable inhibitors of CD45. The

Table 1. Percent inhibition of the *Yersinia* PTPase by selected crude library members at 1 μM concentration[a]

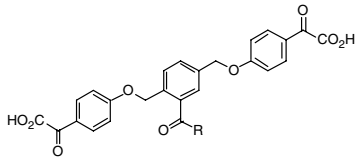

Entry[b]	% Inhibition
A32	95
A59	94
A70	94
A51	91
A93	90
A10	90
A55	90
A8	89
A58	89
A44	87

[a] Assay solutions contained 100 mM acetate buffer at pH 5.5, 1 mM EDTA, 100 mM NaCl, and 10% DMSO.

[b] See Figure 2 for specific structures of the inhibitors.

Table 2. Percent inhibition of PTP1B by selected crude library members at 2 μM concentration[a]

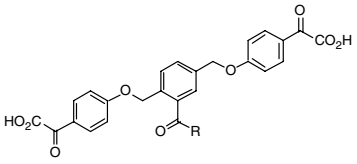

Entry[b]	% Inhibiton
A53	74
A56	63
A32	59
A36	55
A70	51
A98	47
A71	45
A51	39
A10	38
A103	33

[a] Assay solutions contained 100 mM acetate buffer at pH 5.5, 1 mM EDTA, 100 mM NaCl, and 10% DMSO.
[b] See Figure 2 for specific structures of the inhibitors.

selectivity for PTP1B over CD45 ranges from less than a factor of two for compound **11**, to greater than 10-fold for the best PTP1B inhibitor, compound **14**. CD45 also lacks a residue that corresponds to Arg-47 and the residues that constitute the secondary binding site. However, CD45 does contain an Asp residue analogous to Asp-48, while LAR has Asn in its place. If this Asp makes important contacts with the inhibitors, this binding interaction may help to explain the difference in affinities that the inhibitors display for CD45 and LAR. Alternately, the inhibitors may simply bind in a different conformation in the two enzymes.

3. Conclusion

In summary, we have described the parallel synthesis of 104 divalent α-ketocarboxylic acid inhibitors for PTPases. These inhibitors are designed to make contacts with the active site, the secondary binding site, and Arg-47 and Asp-48 of PTP1B. Using this approach, we have discovered an inhibitor that is more than 120 times more potent against PTP1B than compound **2**, the parent structure upon which the library was based. The most potent PTP1B inhibitor in this series, compound **14**, shows excellent selectivity for PTP1B over LAR, 10-fold selectivity over CD45, and less than 2-fold selectivity over TCPTP. Several of the compounds (**12** and **14**) are also potent inhibitors of the *Yersinia* PTPase. We are currently investigating the bioavailability of these and related inhibitors.

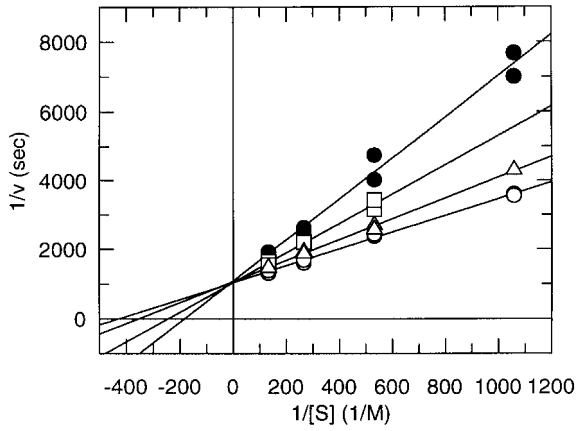

Figure 5. Inhibition of PTP1B by compound **14**. The activity of PTP1B was measured at pH 7.0 as described under the Experimental Section in the presence of the following concentrations of **14**: (○) 0 μM; (Δ) 1.27 μM; (□) 2.54 μM; (●) 3.80 μM. Substrate concentrations used in the assays were 0.94, 1.88, 3.76, and 7.53 mM.

4. Experimental

4.1. General methods

NMR spectra were recorded on Bruker Avance-300 or Avance-400 instruments. Spectra were calibrated using TMS ($\delta = 0.00$ ppm) for ^{1}H NMR, $CDCl_3$ ($\delta = 77.0$ ppm), acetone-d_6 ($\delta = 29.5$ ppm), or DMSO-d_6 ($\delta = 39.5$ ppm) for ^{13}C NMR, and $CFCl_3$ ($\delta = 0.00$ ppm) for ^{19}F NMR. Mass spectra were recorded on either a Shimadzu LCMS-QP8000 or an Applied Biosystems QSTAR electrospray mass spectrometer. HPLC analyses were performed on a Rainin HPLC system with Varian C8 and C18 columns, and UV detection. Semi-preparative HPLC was performed on the same system using a semi-preparative column (21.4 × 250 mm). Reactions were conducted under an atmosphere of dry nitrogen in oven dried glassware. THF was distilled from sodium and benzophenone.

Table 3. Inhibition of phosphatases by compounds **11**–**14**[a]

Compd	IC_{50} (μM)				
	Yersinia PTPase	PTP1B	LAR[b]	CD45	TCPTP
2		73 ± 12			
11	0.51 ± 0.08	4.3 ± 1.0	0% at 650 μM	7.2 ± 0.8	5.3 ± 1.2
12	0.24 ± 0.05	1.5 ± 0.3	0% at 650 μM	6.6 ± 0.9	2.4 ± 0.5
13	0.67 ± 0.15	4.5 ± 1.0	0% at 650 μM	14.2 ± 2.2	5.5 ± 0.9
14	0.27 ± 0.05	0.59 ± 0.07	0% at 200 μM[c]	6.3 ± 2.0	0.96 ± 0.13

[a] Average of two measurements. Assays were performed in 50 mM 3,3-dimethylglutarate buffer at pH 7.0, 1 mM EDTA, 50 mM NaCl, and 10% DMSO.
[b] % Inhibition at the given concentration.
[c] Insoluble beyond this concentration.

Solvents were of reagent grade and were stored over 4 Å molecular sieves. All reagents were used as received. Solvent removal was performed by rotary evaporation at water aspirator pressure.

4.1.1. Compound 6. To a solution of sodium (0.320 g, 13.9 mmol) dissolved in ethanol (40 mL) was added *N*-Boc-D-4-hydroxyphenylglycine methyl ester (**5**,[23] 3.93 g, 13.9 mmol) and then compound **4**[25] (2.33 g, 6.65 mmol). The mixture was stirred at room temperature for 14 h under a N_2 atmosphere, the solvent was removed, and the residue was treated with H_2O (30 mL) and ethyl acetate (30 mL). The layers were separated, and the aqueous layer was extracted with two portions of ethyl acetate (15 mL). The organic layers were combined and washed twice with a saturated solution of aqueous Na_2CO_3 (30 mL), and brine (40 mL), dried over Na_2SO_4, and concentrated to dryness. Purification by flash column chromatography (1:2:6 methylene chloride–ethyl acetate–hexanes) yielded compound **6** (4.60 g, 6.01 mmol, 90%) as colorless foam: ^{1}H NMR (300 MHz, $CDCl_3$) δ 1.23 (t, $J = 7.1$ Hz, 6H), 1.39 (t, $J = 7.1$ Hz, 3H), 1.45 (s, 18H), 4.19 (m, 4H), 4.38 (q, $J = 7.1$ Hz, 2H), 5.10 (s, 2H), 5.25 (d, $J = 7.2$ Hz, 2H), 5.52 (m, 4H), 6.96 (dd, $J = 8.7$, 1.8 Hz, 4H), 7.30 (d, $J = 8.7$ Hz, 2H), 7.31 (d, $J = 8.7$ Hz, 2H), 7.62 (dd, $J = 8.0$, 1.7 Hz, 1H), 7.76 (d, $J = 8.0$ Hz, 1H), 8.10 (d, $J = 1.5$ Hz, 1H); ^{13}C NMR (75 MHz, $CDCl_3$) δ 14.5, 14.7, 28.7, 57.5, 61.7, 62.1 (two overlapping resonances), 68.5, 69.6, 80.5, 115.5 (two overlapping resonances), 128.3, 128.7, 128.8 (two overlapping resonances), 129.9, 130.1, 130.2, 131.9, 136.5, 139.5, 155.2, 158.9, 159.0, 161.7, 171.7, 171.8; HRMS-ESI ($M+H^+$) calcd for $C_{41}H_{53}N_2O_{12}$ 765.3599, found 765.3615.

4.1.2. Compound 7. Compound **6** (1.85 g, 2.67 mmol) was dissolved in a solution of 25% trifluoroacetic acid in methylene chloride (10 mL) and the solution was stirred in an ice bath for 3 h. The solvent was removed, and the residue was taken up in ethyl acetate (30 mL) and washed twice with a saturated solution of aqueous Na_2CO_3 (15 mL) and brine (15 mL). The organic layer was dried over Na_2SO_4 and the solvent was removed by rotary evaporation to yield compound **7** (1.19 g, 2.42 mmol, 91%) as a colorless solid: ^{1}H NMR (300 MHz, DMSO-d_6) δ 1.12 (t, $J = 7.1$ Hz, 6H), 1.25 (t, $J = 7.1$ Hz, 3H), 2.21 (br s, 4H), 4.04 (m, 4H), 4.26 (q, $J = 7.1$ Hz, 2H), 4.43 (s, 2H), 5.16 (s, 2H), 5.38 (s, 2H), 6.92 (d, $J = 8.5$ Hz, 2H), 6.97 (d, $J = 8.5$ Hz, 2H), 7.29 (d, $J = 8.5$ Hz, 4H), 7.66 (s, 2H), 7.96 (s, 1H); ^{13}C NMR (75 MHz, DMSO-d_6) δ 14.8, 14.9, 58.4, 61.1, 61.8, 68.3, 69.1, 115.2, 115.4, 128.9, 129.5, 130.0, 130.1, 132.2, 134.4 (two overlapping resonances), 137.9, 138.4, 158.2, 158.4, 167.3, 175.1; HRMS-ESI ($M+H^+$) calcd for $C_{31}H_{37}N_2O_8$ 565.2550, found 565.2553.

4.1.3. Compound 9. Compound **7** (0.291 g, 0.515 mmol) was suspended in a solution of 2.5 M NaOH (10 mL) and the mixture was heated at reflux for 4 h. After cooling, the resulting solution was acidified to pH 7 with 3 M HCl and the precipitate (compound **8**) was collected by centrifugation. Without further purification, trifluoroacetic anhydride (20 mL) was added in two portions to compound **8** and the mixture was heated at reflux for 4 h, then concentrated to dryness. The residue was treated with ethyl acetate (30 mL) and the insoluble material was removed by filtration. The filtrate was evaporated and the remaining material was purified by flash chromatography (1:1:2 chloroform–ethyl acetate–hexanes) to give compound **9** (0.248 g, 0.390 mmol, 76%) as a colorless solid: ^{1}H NMR (300 MHz, DMSO-d_6) δ 5.33 (s, 2H), 5.59 (s, 2H), 7.05 (q, $J = 4.5$ Hz, 2H), 7.22 (d, $J = 8.9$ Hz, 2H), 7.26 (d, $J = 8.9$ Hz, 2H), 7.70 (m, 2H), 8.06 (s, 1H), 8.30 (d, $J = 8.7$ Hz, 4H), 13.25 (br s, 1H); ^{13}C NMR (75 MHz, DMSO-d_6) δ 68.7, 69.6, 92.3 (q, $J_{CF} = 33.2$ Hz), 116.2, 116.4, 121.0 (two overlapping resonances), 121.8 (q, $J_{CF} = 280$ Hz), 129.3, 130.6, 130.7, 131.5, 131.6, 132.2, 137.2, 138.1, 159.8, 163.2, 163.4, 164.2, 168.7; ^{19}F NMR (376 MHz, DMSO-d_6) δ −78.5 (t, $J = 4.1$ Hz); HRMS-ESI ($M-H^+$, negative ion mode) calcd for $C_{29}H_{17}F_6N_2O_8$ 635.0889, found 635.0902.

4.2. General experimental for the synthesis of the library

To a suspension of compound **9** (40 mg, 62.8 μmol) in benzene (3 mL) was added $SOCl_2$ (0.5 mL). The mixture was heated at reflux for 3 h under a N_2 atmosphere, then the solvents were removed under vacuum. The residue was dissolved in methylene chloride and split into eight equal portions. Each portion was added to a solution of a different aromatic amine (2.2 equiv) dissolved in either CH_2Cl_2 or THF. See Figure 2 for a list of aromatic amines that were used in this reaction. The reaction was stirred overnight at 4 °C and the solvent was removed. Without further purification, a solution of 0.25 M NaOH (0.5 mL) was added and the mixture was stirred for 2 h. The reaction was quenched with 0.5 M HCl (1.5 mL) and the precipitate was collected by centrifugation. After washing the solid twice with 0.1 M HCl, the solid was resuspended in water (0.5 mL) and extracted twice with EtOAc (0.5 mL). The organic layers were combined, dried over Na_2SO_4, and concentrated to dryness.

4.2.1. Compound 10a. To a suspension of compound **9** (70.7 mg, 0.111 mmol) in benzene (4 mL) was added $SOCl_2$ (1 mL). The mixture was heated at reflux for 3 h under a N_2 atmosphere, then the solvents were removed under vacuum. The residue was dissolved in methylene chloride (1.5 mL) and a solution 1-aminonaphthalene (39.8 mg, 0.278 mmol) in methylene chloride (0.25 mL) was added. The solution was stirred at 4 °C overnight, diluted with methylene chloride (25 mL), and washed twice with 1 N HCl (15 mL). The organic layer was dried over Na_2SO_4, concentrated to dryness, and the residue was washed twice with benzene to yield compound **10a** (50.9 mg, 66.9 μmol, 60%) as a colorless solid: ^{1}H NMR (300 MHz, acetone-d_6) δ 5.42 (s, 2H), 5.62 (s, 2H), 6.82 (m, 2H), 7.27 (d, $J = 9.0$ Hz, 2H), 7.33 (d, $J = 8.5$ Hz, 2H), 7.51 (m, 3H), 7.79 (m, 3H), 7.91 (d, $J = 7.4$ Hz, 1H), 7.96 (dd, $J = 7.4$, 2.0 Hz, 1H), 8.13 (s, 1H), 8.22

(d, $J = 8.1$ Hz, 1H), 8.39 (d, $J = 9.0$ Hz, 2H), 8.44 (d, $J = 9.0$ Hz, 2H), 9.78 (s, 1H); ^{13}C NMR (75 MHz, acetone-d_6) δ 68.2, 69.7, 92.4 (q, $J_{CF} = 34.0$ Hz), 115.8, 121.0, 121.1, 121.5 (q, $J_{CF} = 280$ Hz), 122.9, 123.0, 125.9, 126.4, 126.5, 127.7, 128.7, 129.0, 129.7, 129.9, 131.3 (two overlapping resonances), 133.9, 134.7, 135.6, 136.8, 137.3, 159.9, 163.5, 163.6, 163.7, 168.0; HRMS-FAB (M+Na$^+$) calcd for $C_{39}H_{25}F_6NaN_3O_7$ 784.1494, found 784.1477.

4.2.2. Compound 10b. To a suspension of compound **9** (43.8 mg, 68.8 μmol) in benzene (3 mL) was added $SOCl_2$ (0.5 mL). The mixture was heated at reflux for 3 h under a N_2 atmosphere, then the solvents were removed under vacuum. The residue was dissolved in methylene chloride (1 mL) and a solution of 4-phenoxyaniline (31.5 mg, 170 μmol) in methylene chloride (0.25 mL) was added. The solution was stirred at 4 °C overnight, diluted with methylene chloride (15 mL), and washed twice with 1 N HCl (15 mL). The organic layer was dried over Na_2SO_4, concentrated to dryness, and the residue was purified by flash chromatography (1:2 EtOAc–hexanes) to yield compound **10b** (44.8 mg, 55.8 μmol, 81%) as a colorless solid: ^{1}H NMR (300 MHz, acetone-d_6) δ 5.37 (s, 2H), 5.57 (s, 2H), 6.81 (m, 2H), 7.01 (d, $J = 8.8$ Hz, 2H), 7.03 (d, $J = 8.9$ Hz, 2H), 7.12 (t, $J = 7.5$ Hz, 1H), 7.23 (d, $J = 9.0$ Hz, 2H), 7.29 (d, $J = 9.0$ Hz, 2H), 7.38 (d, $J = 7.5$ Hz, 1H), 7.40 (d, $J = 7.5$ Hz, 1H), 7.71 (dd, $J = 7.9$, 1.3 Hz, 1H), 7.76 (d, $J = 7.9$ Hz, 1H), 7.83 (d, $J = 9.0$ Hz, 2H), 7.89 (s, 1H), 8.37 (d, $J = 9.0$ Hz, 2H), 8.43 (d, $J = 9.0$ Hz, 2H), 9.76 (s, 1H); ^{13}C NMR (75 MHz, acetone-d_6) 68.0, 69.6, 92.4 (q, $J_{CF} = 34.3$ Hz), 115.8 (two overlapping resonances), 118.5, 119.8, 121.0, 121.1, 121.5 (q, $J_{CF} = 280$ Hz), 122.0, 123.4, 127.3, 129.4, 129.9, 130.2, 131.2, 131.3, 135.5 (two overlapping resonances), 136.8, 137.1, 153.4, 158.2, 159.8, 163.5, 163.6, 163.7, 167.0; HRMS-FAB (M+Na$^+$) calcd for $C_{41}H_{27}F_6NaN_3O_8$ 826.1600, found 826.1580.

4.2.3. Compound 10c. Compound **10c** was prepared from compound **9** and 4-aminobenzophenone by procedures analogous to the preparation of **10b** except that flash chromatography was performed with 1:3 EtOAc–hexanes. **10c** (29.4 mg, 36 μmol, 71%): ^{1}H NMR (300 MHz, acetone-d_6) δ 5.37 (s, 2H), 5.58 (s, 2H), 6.81 (m, 2H), 7.22 (d, $J = 9.0$ Hz, 2H), 7.29 (d, $J = 9.0$ Hz, 2H), 7.57 (t, $J = 7.3$ Hz, 1H), 7.67 (t, $J = 7.3$ Hz, 1H), 7.74 (d, $J = 8.1$ Hz, 1H), 7.79 (m, 3H), 7.83 (d, $J = 8.7$ Hz, 2H), 7.99 (d, $J = 8.7$ Hz, 2H), 7.94 (s, 1H), 8.37 (d, $J = 8.9$ Hz, 2H), 8.43 (d, $J = 8.9$ Hz, 2H), 10.09 (s, 1H); ^{13}C NMR (75 MHz, acetone-d_6) δ 68.0, 69.6, 92.4 (q, $J_{CF} = 34.3$ Hz), 115.8, 119.4, 121.1 (two overlapping resonances), 121.5 (q, $J_{CF} = 280$ Hz), 127.4, 128.7, 129.5, 129.9, 130.2, 131.2, 131.3, 131.5, 132.5, 133.1, 135.7, 136.4, 137.3, 138.5, 143.6, 159.8, 163.5, 163.7, 167.6, 194.9; HRMS-FAB (M+Na$^+$) calcd for $C_{42}H_{27}F_6NaN_3O_8$ 838.1600, found 838.1582.

4.2.4. Compound 10d. Compound **10d** was prepared from compound **9** and 1-aminopyrene by procedures analogous to the preparation of **10a**. **10d** (49.4 mg, 59.1 μmol, 82%): ^{1}H NMR (300 MHz, DMSO-d_6) δ 5.42 (s, 2H), 5.56 (s, 2H), 7.06 (m, 2H), 7.28 (d, $J = 8.9$ Hz, 2H), 7.35 (d, $J = 9.0$ Hz, 2H), 7.75 (m, 2H), 8.10 (m, 3H), 8.20 (m, 3H), 8.31 (m, 8 H), 10.99 (s, 1H); ^{13}C NMR (75 MHz, DMSO-d_6) δ 68.5, 69.9, 92.3 (q, $J_{CF} = 33.3$ Hz), 116.3, 116.4, 121.0, 121.1, 121.8 (q, $J_{CF} = 280$ Hz), 124.6, 125.2, 125.5, 125.7, 125.9, 126.0, 126.2, 127.3, 127.8, 128.0, 128.1, 128.6, 129.2, 129.7, 130.4, 130.5, 131.3, 131.6 (two overlapping resonances), 132.3, 132.5, 135.3, 137.2, 137.5, 158.8, 163.4, 163.5, 164.2, 168.7; HRMS-FAB (M+Na$^+$) calcd for $C_{45}H_{27}F_6NaN_3O_7$ 858.1651, found 858.1636.

4.3. Representative procedure for the synthesis of compounds 11–14

4.3.1. Compound 12. A solution of 0.25 M NaOH (1 mL) was added to compound **10b** (11.1 mg, 13.8 μmol) and the mixture was stirred at room temperature for 1 h. The solution was washed twice with Et_2O and the aqueous layer was acidified with 0.5 M HCl to approximately pH 2. The precipitate was collected by centrifugation and then resuspended in water (1 mL). Addition of ethyl acetate (1 mL) dissolved the precipitate and after the layers were separated, the aqueous layer was extracted once with ethyl acetate (1 mL). The ethyl acetate layer was dried over Na_2SO_4 and concentrated to dryness to yield compound **12** as a yellow solid (5.8 mg, 8.99 μmol, 65%): ^{1}H NMR (300 MHz, acetone-d_6) δ 5.37 (s, 2H), 5.57 (s, 2H), 7.01 (d, $J = 8.6$ Hz, 2H), 7.03 (d, $J = 8.9$ Hz, 2H), 7.12 (t, $J = 7.4$ Hz, 1H), 7.20 (d, $J = 8.9$ Hz, 2H), 7.26 (d, $J = 8.9$ Hz, 2H), 7.38 (d, $J = 8.3$ Hz, 1H), 7.40 (d, $J = 8.5$ Hz, 1H), 7.70 (dd, $J = 7.9$, 1.4 Hz, 1H), 7.78 (d, $J = 8.0$ Hz, 1H), 7.82 (d, $J = 8.9$ Hz, 2H), 7.88 (s, 1H), 8.02 (d, $J = 8.8$ Hz, 2H), 8.07 (d, $J = 8.9$ Hz, 2H), 9.76 (s, 1H); ^{13}C NMR (75 MHz, acetone-d_6) δ 68.1, 69.7, 115.7 (two overlapping resonances), 118.5, 119.8, 121.9, 123.4, 126.0 (two overlapping resonances), 127.4, 129.4, 129.9, 130.2, 132.6, 132.7, 135.4, 135.5, 136.7, 137.0, 153.4, 158.2, 164.5 (two overlapping resonances), 165.3, 167.0, 186.0; LRMS-ESI (M−H$^+$, negative ion mode) calcd for $C_{37}H_{26}NO_{10}$ 644, found 644.

4.3.2. Compound 11. (6.3 mg, 10 μmol, 70%): ^{1}H NMR (300 MHz, acetone-d_6) δ 5.43, (s, 2H), 5.62 (s, 2H), 7.27 (m, 4H), 7.51 (m, 3H), 7.79 (m, 3H), 7.90 (d, $J = 7.4$ Hz, 1H), 7.96 (d, $J = 7.4$ Hz, 1H), 8.07 (m, 5H), 8.20 (d, $J = 7.9$ Hz, 1H), 9.78 (s, 1H); ^{13}C NMR (75 MHz, acetone-d_6) δ 68.3, 69.8, 115.7, 122.8, 123.0, 125.9 (two overlapping resonances), 126.0, 126.4, 126.5, 127.7, 128.7, 128.9, 129.7, 130.0, 132.7 (two overlapping resonances), 133.8, 134.7, 135.5, 136.8, 137.2, 164.5, 164.6, 165.2, 167.9, 186.0; LRMS-ESI (M−H$^+$, negative ion mode) calcd for $C_{35}H_{24}NO_9$ 602, found 602.

4.3.3. Compound 13. (12.3 mg, 18.7 μmol, 52%): ^{1}H NMR (300 MHz, acetone-d_6) δ 5.39 (s, 2H), 5.59 (s, 2H), 7.20 (d, $J = 9.0$ Hz, 2H), 7.27 (d, $J = 9.0$ Hz, 2H), 7.57

(t, $J = 7.3$ Hz, 2H), 7.67 (t, $J = 7.3$ Hz, 1H), 7.78 (m, 4H), 7.83 (d, $J = 8.8$ Hz, 2H), 7.93 (s, 1H), 8.00 (m, 4H), 8.07 (d, $J = 9.0$ Hz, 2H), 10.08 (s, 1H); ^{13}C NMR (75 MHz, acetone-d_6) δ 68.1, 69.7, 115.7 (two overlapping resonances), 119.4 (two overlapping resonances), 126.0, 126.1, 127.5, 128.7, 129.5, 129.9, 130.2, 131.5, 132.5, 132.6, 132.7, 133.1, 135.6, 136.4, 137.2, 164.4, 165.3, 167.6, 186.1, 194.9; LRMS-ESI ($M-H^+$, negative ion mode) calcd for $C_{38}H_{26}NO_{10}$ 656, found 656.

4.3.4. Compound 14. (21.1 mg, 31.1 μmol, 53%): ^{1}H NMR (300 MHz, DMSO-d_6) δ 5.43 (s, 2H), 5.57 (s, 2H), 7.30 (m, 4H), 7.74 (m, 2H), 7.95 (m, 3H), 8.09 (m, 3H), 8.18 (m, 3H), 8.31 (m, 5H), 10.99 (s, 1H); ^{13}C NMR (75 MHz, DMSO-d_6) δ 68.6, 70.0, 116.3, 116.4, 123.6, 124.6, 125.2, 125.5, 125.7, 125.8, 125.9, 126.1, 126.2, 127.3, 127.8, 128.0, 128.1, 128.7, 129.8, 130.3, 130.5, 131.3, 131.6, 132.2, 133.0, 135.2, 137.3, 137.4, 159.8, 164.5, 164.6, 167.3, 168.2, 168.7, 187.9; LRMS-ESI ($M-H^+$, negative ion mode) calcd for $C_{41}H_{26}NO_9$ 676, found 676.

4.4. PTPase assays

The phosphatase activities of the *Yersinia* PTPase, PTP1B, LAR, TCPTP, and CD45 (all purchased from Calbiochem) were assayed using *p*-NPP as the substrate at 25 °C and the reaction progress was monitored by UV spectroscopy. Initial rates were determined by monitoring the hydrolysis of *p*-NPP at 405 nm, from 30 to 150 s after mixing. Percent inhibition assay solutions contained 100 mM acetate at pH 5.5, 1 mM EDTA, 100 mM NaCl, and 10% DMSO. Substrate concentrations were kept at 2.5 and 1.2 mM for the *Yersinia* PTPase and PTP1B assays, respectively. The K_m values under these conditions for the *Yersinia* PTPase and PTP1B were found to be 2.5 and 0.62 mM, respectively. IC_{50} assay solutions contained substrate at K_m concentration, 50 mM 3,3-dimethylglutarate at pH 7.0, 1 mM EDTA, 50 mM NaCl, and 10% DMSO. The K_m values under these conditions for the *Yersinia* PTPase, PTP1B, LAR, TCPTP, and CD45 were found to be 2.7, 2.0, 2.3, 2.1, and 7.0 mM, respectively. IC_{50} values were calculated using a Dixon analysis. Data analysis was performed with the commercial graphing package Grafit (Erithacus Software Ltd).

4.5. Molecular modeling

Molecular modeling studies were performed using Insight II version 2000.1 (Accelrys, 9685 Scranton Rd., San Diego, CA 92121) running on a SGI workstation. The coordinates from the crystal structure of PTP1B in complex with [4-{4-[4-(difluorophosphonomethyl)-phenyl]butyl}phenyl)difluoromethyl]phosphonic acid (PDB entry 1KAV) were used as the starting point for calculations. Hydrogen atoms were added where necessary, charges were fixed, and the calculations were performed using the Discover module and the cvff force field. Compound **2** was constructed using the Builder module and manually docked into the active site using the ligand that was present in the original structure as the basis for initial placement. This system was minimized with 1000 iterations of conjugate gradient minimization.

Acknowledgements

This research was supported by the NIH NIGMS (Grant R01 GM057327). We thank Professor David Cane for use of the SGI workstation.

References and notes

1. Hunter, T. *Cell* **2000**, *100*, 113.
2. Zhang, Z.-Y. *Curr. Opin. Chem. Biol.* **2001**, *5*, 416.
3. Goldstein, B. J.; Li, P.-M.; Ding, W.; Ahmad, F.; Zhang, W.-R. *Vitam. Horm.* **1998**, *54*, 67.
4. Elchebly, M.; Payette, P.; Michaliszyn, E.; Cromlish, W.; Collins, S.; Loy, A. L.; Normandin, D.; Cheng, A.; Himms-Hagen, J.; Chan, C.-C.; Ramachandran, C.; Gresser, M. J.; Tremblay, M. L.; Kennedy, B. P. *Science* **1999**, *283*, 1544.
5. Klaman, L. D.; Boss, O.; Peroni, O. D.; Kim, J. K.; Martino, J. L.; Zabolotny, J. M.; Moghal, N.; Lubkin, M.; Kim, Y.-B.; Sharpe, A. H.; Stricker-Krongrad, A.; Shulman, G. I.; Neel, B. G.; Kahn, B. B. *Mol. Cell. Biol.* **2000**, *20*, 5479.
6. van Huijsduijnen, R. H.; Bombrun, A.; Swinnen, D. *Drug Discov. Today* **2002**, *7*, 1013.
7. Thomas, M. L.; Brown, E. J. *Immunol. Today* **1999**, *20*, 406.
8. Bliska, J. B.; Guan, K. L.; Dixon, J. E.; Falkow, S. *Proc. Natl. Acad. Sci. U.S.A.* **1991**, *88*, 1187.
9. Burke, T. R., Jr.; Zhang, Z.-Y. *Biopolymers* **1998**, *47*, 225.
10. Jia, Z.; Barford, D.; Flint, A. J.; Tonks, N. K. *Science* **1995**, *268*, 1754.
11. Vetter, S. W.; Keng, Y.-F.; Lawrence, D. S.; Zhang, Z.-Y. *J. Biol. Chem.* **2000**, *275*, 2265.
12. Puius, Y. A.; Zhao, Y.; Sullivan, M.; Lawrence, D. S.; Almo, S. C.; Zhang, Z.-Y. *Proc. Natl. Acad. Sci. U.S.A.* **1997**, *94*, 13420.
13. Salmeen, A.; Andersen, J. N.; Myers, M. D.; Tonks, N. K.; Barford, D. *Mol. Cell* **2000**, *6*, 1401.
14. Taing, M.; Keng, Y.-F.; Shen, K.; Wu, L.; Lawrence, D. S.; Zhang, Z.-Y. *Biochemistry* **1999**, *38*, 3793.
15. Shen, K.; Keng, Y.-F.; Wu, L.; Guo, X.-L.; Lawrence, D. S.; Zhang, Z.-Y. *J. Biol. Chem.* **2001**, *276*, 47311.
16. Jia, Z.; Ye, Q.; Dinaut, A. N.; Wang, Q.; Waddleton, D.; Payette, P.; Ramachandran, C.; Kennedy, B.; Hum, G.; Taylor, S. D. *J. Med. Chem.* **2001**, *44*, 4584.
17. Guo, X.-L.; Shen, K.; Wang, F.; Lawrence, D. S.; Zhang, Z.-Y. *J. Biol. Chem.* **2002**, *277*, 41014.
18. Sun, J.-P.; Fedorov, A. A.; Lee, S.-Y.; Guo, X.-L.; Shen, K.; Lawrence, D. S.; Almo, S. C.; Zhang, Z.-Y. *J. Biol. Chem.* **2003**, *278*, 12406.
19. Asante-Appiah, E.; Patel, S.; Dufresne, C.; Roy, P.; Wang, Q.; Patel, V.; Friesen, R. W.; Ramachandran, C.; Becker, J. W.; Leblanc, Y.; Kennedy, B. P.; Scapin, G. *Biochemistry* **2002**, *41*, 9043.
20. Szczepankiewicz, B. G.; Liu, G.; Hajduk, P. J.; Abad-Zapatero, C.; Pei, Z.; Xin, Z.; Lubben, T. H.; Trevillyan, J. M.; Stashko, M. A.; Ballaron, S. J.; Liang, H.; Huang, F.; Hutchins, C. W.; Fesik, S. W.; Jirousek, M. R. *J. Am. Chem. Soc.* **2003**, *125*, 4087.

21. Chen, Y. T.; Onaran, M. B.; Doss, C. J.; Seto, C. T. *Bioorg. Med. Chem. Lett.* **2001**, *11*, 1935.
22. Chen, Y. T.; Xie, J.; Seto, C. T. *J. Org. Chem.* **2003**, *68*, 4123.
23. Chen, Y. T.; Seto, C. T. *J. Med. Chem.* **2002**, *45*, 3946.
24. Barnish, I. T.; Cross, P. E.; Danilewicz, J. C.; Dickinson, R. P.; Stopher, D. A. *J. Med. Chem.* **1981**, *24*, 399.
25. Benniston, A. C.; Harriman, A. *Synlett* **1993**, *3*, 223.
26. van Huijsduijnen, R. H. *Gene* **1998**, *225*, 1.
27. Xin, Z.; Oost, T. K.; Abad-Zapatero, C.; Hajduk, P. J.; Pei, Z.; Szczepankiewicz, B. G.; Hutchins, C. W.; Ballaron, S. J.; Stashko, M. A.; Lubben, T.; Trevillyan, J. M.; Jirousek, M. R.; Liu, G. *Bioorg. Med. Chem. Lett.* **2003**, *13*, 1887.
28. Pei, Z.; Li, X.; Liu, G.; Abad-Zapatero, C.; Lubben, T.; Zhang, T.; Ballaron, S. J.; Hutchins, C. W.; Trevillyan, J. M.; Jirousek, M. R. *Bioorg. Med. Chem. Lett.* **2003**, *13*, 3129.
29. Tsai, A. Y. M.; Itoh, M.; Streuli, M.; Thai, T.; Saito, H. *J. Biol. Chem.* **1991**, *266*, 10534.
30. Saito, H.; Streuli, M.; Krueger, N. X.; Itoh, M.; Tsai, A. Y. M. *Biochem. Soc. Trans.* **1992**, *20*, 165.